Pseudopotential calculations of positron annihilation rates in bubbles of the heavier noble gases contained in copper

1990 J. Phys.: Condens. Matter 2 10529

(http://iopscience.iop.org/0953-8984/2/51/024)

J. Phys.: Condens. Matter 2 (1990) 10529–10547. Printed in the UK

Pseudopotential calculations of positron annihilation rates in bubbles of the heavier noble gases contained in copper

G M Dunn†, P Rice-Evans† and J H Evans‡

† Physics Department, Royal Holloway and Bedford New College, University of London, Egham Hill, Egham, Surrey, TW20 OEX, UK

‡ Materials Development Division, Harwell Laboratory, Oxon, OX11 ORA, UK

Received 2 April 1990, in final form 2 August 1990

Abstract. A pseudopotential technique has been applied to calculate lifetimes for positron annihilation in copper defected with bubbles of the noble gases Ne, Ar, Kr and Xe at various gas densities. The positron in each case was found to be in a surface state of the metal on the interior surface of the bubble, the wavefunction deviating slightly from a perfect surface state according to the strength of the attractive polarization potential from the gas atoms in the bubble. This effect was particularly noticeable in the case of xenon where the surface annihilation rate was reduced to about 40% of the perfect surface state.

1. Introduction

Positron annihilation techniques (PAT) are well established tools for the study of defects within all types of materials in the solid phase. The positrons, finding the defects attractive due to their lack of positive charge, annihilate preferentially in the defects. Their lifetime and Doppler shifted annihilation radiation provide valuable information about the electron density and velocity distribution in this environment. Among the defects that can be studied in this way are the bubbles formed due to the precipitation of noble gas atoms in metals and interesting experimental results have already been reported (for example see Jensen 1988, Nieminen 1989). To the materials scientist, noble gas behaviour in metals is of continuing interest, due partly to the potential of the helium for causing metal embrittlement (important when helium is produced by (n,α) reactions under neutron irradiation), and due to more general effects in processes such as sputter cleaning and ion beam mixing. In addition, fundamental aspects have received attention (Ullmaier 1983) with recent emphasis being paid to the heavier noble gases which can be found precipitated in the solid phase (Evans 1985).

With respect to theory, quantitative calculation of positron annihilation rates in small vacancy clusters decorated with noble gases were first performed by Hansen *et al* (1984) using the method of Puska and Nieminen (1983). The procedure which involves solving the three-dimensional Schrödinger equation over a section of the lattice incorporating the defect is difficult to apply to larger defects like bubbles because of problems of positioning the noble gas atoms (the gas is often fluid), but primarily because the calculations quickly become too large, except for those with access to the largest computers. Jensen and Nieminen (1987) used a model which assumed that the

0953-8984/90/5110529+19$03.50

potential deep inside the bubble did not significantly change the surface state of the positron and as such solved only for a single layer of gas on the metal surface. The annihilation rate of a trapped positron was then found by adding the constant surface annihilation rate with the free electrons of the metal host to the annihilation rate off each gas atom as a function of distance from the metal surface. (The density of gas atoms as a function of distance from the metal was found by means of a molecular dynamics simulation). In this way a characteristic annihilation rate was found as a function of the gas density. If the density is known, the gas pressure is known, and so an estimate of bubble size can be made. Their calculations on krypton and helium performed in this manner agreed very favourably with other more lengthy calculations they performed for a surface with multiple layers of gas, in order to validate their initial assumption.

We, Dunn *et al* (1990a), found that the use of pseudopotentials also produced accurate results when applied to the evaluation of bubbles of He gas in various metals. The use of pseudopotentials greatly speeds up the rate of calculation, reducing the problem to the solving of several one-dimensional Schrödinger equations. Pseudopotentials also allow for the evaluation over much larger bubbles than the Puska–Nieminen method, solve the problem in the correct symmetry and allow the potential of the gas atoms to be represented deep inside the bubble.

In this paper we have applied the pseudopotential method to the calculations of lifetimes for bubbles of Ne, Ar, Kr and Xe in copper over a range of densities corresponding to pressures up to the order of 5×10^9 Pa (corresponding to the maximum pressure likely to be found in such bubbles) at a temperature of 300 K. In addition, we compare the results for Kr with the experimental and more lengthy theoretical calculations of Jensen and Nieminen (1987) and show our results to be in excellent agreement with theirs.

2. Methods

2.1. Molecular dynamics simulations

In order to find the average configuration of the trapped gas atoms within the bubbles we performed molecular dynamics simulations, the simulation being of a standard particle–particle (P^2) type (Hockney and Eastwood 1983). The particles were positioned initially in a FCC structure in a bubble in a jellium host, the bubble radius usually being about 15 Å (we found little difference in the resulting profile away from the jellium if larger bubble sizes were used). The particles were then moved under the potentials of each other and of the host over several thousand time steps of about 5 fs (5×10^{-15} s), the average atom configuration being built up after the assembly had established itself at the desired temperature (300 K).

For the gas–gas potential a standard 6–12 Lennard-Jones potential was used†

$$V(r) = 4\epsilon\left[\left(\frac{\sigma}{r}\right)^{12} - \left(\frac{\sigma}{r}\right)^{6}\right]. \tag{1}$$

† All calculations and results unless otherwise stated are expressed in atomic units with Ryd as the unit of energy (1 Ryd = (1/2) Hartree = 13.6 eV = 2.17×10^{-18} J). Values for density are expressed in atoms au^{-3} (1 atom au^{-3} = 6.79×10^{30} atoms m^{-3}).

Table 1. Values of constants used for the potentials in the molecular dynamics simulations. The units are eV for energy (apart from ϵ) and au for length.

Gas	C_{VW}	Z_{VW}	K_c	α	HKS α	ϵ (K)	σ
Ne	3.04	0.4044	0.75	700	800	36	5.18
Ar	10.12	0.4889	0.73	1600	1700	121	6.43
Kr	14.23	0.5170	0.72	2700	—	163	6.91
Xe	20.81	0.5584	0.71	3800	—	231	7.54

(In order to increase the speed of the program we did not consider particles at a greater distance than 2σ atomic units from each other to have any interaction.) Values for σ and ϵ are given in table 1 from Bernardes (1958).

The host surface potential is composed of a strong repulsive component which to a good approximation (Manninen *et al* 1984) is proportional to the electron density at the site of the gas atom, and of a much weaker attractive van der Waals potential. The repulsive component of the potential is given by

$$V_e(z) = \frac{\alpha n_0}{[\exp(zF/\lambda_F) + 1]} \tag{2}$$

where α is the constant of proportionality and the rest of the term is a parametrization of the Lang–Kohn (1973) surface electron densities, n_0 being the host free electron density, λ_F the wavelength of an electron at the hosts Fermi surface and F is a constant factor which for copper has a value of about 10.4.

The attractive van der Waals force is given by Norlander and Harris (1984) to be

$$V_{VW}(z_n) = \frac{C_{VW}}{(Z_n - Z_{VW})^3} f(k_c(Z_n - Z_{VW})) \tag{3}$$

where

$$f(x) = 1 - [2x(1+x) + 1]\exp(-2x)\,. \tag{4}$$

Z_n is the distance to the host jellium, Z_{VW},C_{VW} and k_c are constants (Zaremba and Kohn 1975) given in table 1.

The values of α and K_c are somewhat nebulous. The origin of K_c is that of a cut-off wavevector in the evaluation of the van der Waals potential and is known to be of the order of the inverse of the size of the atom (Zaremba and Kohn 1975). Values for α may be evaluated using HKS density functional theory. This involves solving for a system of N electrons, N Schrödinger-type equations, the potential term in each equation being the electrostatic potential of all the other electrons along with an effective exchange potential dependant upon the electron density. The procedure becomes difficult to apply for heavy atoms and so values of α at present only exist for the lighter noble gas atoms, see for example Stott and Zaremba (1979) for He and Puska *et al* (1981) for Ne and Ar. We are therefore in the position of having to estimate values of α for Kr and Xe. We have done this using the Thomas–Fermi approximation rather than the superposition scheme of Gordon and Kim (see Clugson 1978), the Gordon–Kim method only being suitable for calculations on closed shell atoms and not metals.

3. Thomas–Fermi approximation

3.1. Thomas–Fermi estimates of α

It is known (see March 1957) that the potentials and binding energies of atoms may be estimated with resonable accuracy by making use of the Thomas–Fermi approximation wherein the electron density at each point in the atom is assumed to represent a free electron system, the electrons stacking up to the local chemical potential at that point so that

$$E_F(\boldsymbol{r}) = (3\pi^2 n_-(\boldsymbol{r}))^{2/3} = V(\boldsymbol{r}) = V_p(\boldsymbol{r}) + V_c \tag{5}$$

where $V_p(r)$ is a potential which varies from point to point, V_c is any constant component (for an atom adsorbed in a jellium this component would be approximately $(3\pi^2 n_e)^{2/3}$), $E_F(\boldsymbol{r})$ is the local Fermi surface and n_- (n_+) is the density of negative (positive) charges. Taken together with Poisson's equation

$$\nabla^2 V(\boldsymbol{r}) = -8\pi(n_+(\boldsymbol{r}) - n_-(\boldsymbol{r})) \tag{6}$$

we obtain (in spherical co-ordinates)

$$\frac{d^2 V_p(r)}{dr^2} = \frac{8}{3\pi}[(V_p(r) + V_c)^{3/2} - V_c^{3/2}] - \frac{2}{r}\frac{dV_p(r)}{dr} \tag{7}$$

This non-linear differential equation was solved by using continuous analytic continuation with the boundary conditions

$$V_p(r) = \begin{cases} (2Z/r) + V_-(r) & \text{as } r \to 0 \\ 0 & \text{as } r \to \infty \end{cases}$$

$$\frac{dV_p(r)}{dr} = \begin{cases} -(2Z/r^2) & \text{as } r \to 0 \\ 0 & \text{as } r \to \infty \end{cases}$$

where $V_-(r)$ (the net potential from the distribution of electrons) was varied until all the other boundary conditions were satisfied.

The binding energy of the resulting system may then be calculated by summing the electrostatic, kinetic and exchange energies

$$E_{be} = ZV_c + \int V_c n(\boldsymbol{r})\,d\boldsymbol{r} + \int E_{n_-} n_-(\boldsymbol{r})\,d\boldsymbol{r} + \iint \frac{n(\boldsymbol{r})n(\boldsymbol{r}')\,d\boldsymbol{r}'\,d\boldsymbol{r}}{|\boldsymbol{r} - \boldsymbol{r}'|} + \int \frac{2Zn(\boldsymbol{r})\,d\boldsymbol{r}}{|\boldsymbol{r} - \boldsymbol{R}_z|} \tag{8}$$

where Z is the atomic number of the adsorbed atom, $n(\boldsymbol{r})$ is the total charge density and $n_-(\boldsymbol{r})$ is the density of electrons. The summation is carried out over a volume of jellium which is large enough for the electron density to reach its normal density in the jellium away from the adsorbed atom. The kinetic energy term is given by

$$E_{n_-} = \begin{cases} 2.21 r_s^{-2} - 0.916 r_s^{-1} - 0.88(r_s + 7.8)^{-1} & \text{if } r_s \geq 1 \\ 2.21 r_s^{-2} - 0.916 r_s^{-1} - 0.062 \log_e(r_s) - 0.096 & \text{if } r_s < 1 \end{cases}$$

Table 2. The constants η, A and B in equations (41), (42) and (44) and β and r_0 of Schrader's free atom polarization potentials. a is the lattice translation vector of a unit cell of crystal at the solid uncompressed density of the material. τ is the experimental lifetime and γ the average enhancement factor required to reproduce this rate.

Gas	η	A	B	β	r_0	a (FCC)	τ exp.	Z_{eff}	γ
Ne	18	410	100	2.663	1.9	8.37	345	8.16	3
Ar	36	631	545	11.06	2.23	9.93	420	12.6	3.1
Kr	42	830	814	16.74	2.37	10.81	400	16.5	3.73
Xe	70	1030	1382	27.29	2.54	11.71	400	20	4

(see for example Clugson (1978); several more sophisticated local kinetic energy functionals now exist and the interested reader wishing to do a more thorough calculation is referred to Plumer and Stott (1985)). The heat of adsorption is then the difference between the binding energies of the jellium and free atom, and the energy of the adsorbed atom system.

As might be expected from such a crude approximation the values for alpha determined using the Thomas–Fermi approximation were not accurate, yielding results almost twice the size of those for He, Ne and Ar found using HKS density functional theory. The heats of adsorption in each case did, however, increase linearly with electron density and the ratios of the Thomas–Fermi α values for He, Ne and Ar were almost the same as those determined using HKS theory. We therefore thought it reasonable to scale down the Thomas–Fermi α values for Kr and Xe according to the amount that the He, Ne and Ar values had to be scaled down in order to bring them into line with the HKS values.

The values for α used in the molecular dynamics simulations are given in table 2.

3.2. Choice of potential

Having determined approximate values for α, we must now estimate values for K_c.

The primary function of K_c, the cut-off wavenumber in equation (3), is to prevent the collapse of the backwall of the potential. In the case of helium, the term involving K_c does not really interfere too much with the van de Waals inverse cube relation at the equilibrium position (Norlander and Harris 1984). For the purposes of this work we have assumed that this will also be the case for the other noble gases. K_c has therefore been chosen to be greater than 0.5 au^{-1}.

The values of α and K_c are then varied slightly until a potential well of the proposed universal shape (Vidali *et al* 1983) is formed.

All this may sound rather vague, but as noted by us earlier (Dunn *et al* 1990), any reasonable combination of values for α and K_c such that the potential well has a minimum of about the correct value and that the backwall of the potential increases monotonically into the jellium (as is believed to be the case (Norlander and Harris 1984) produce much the same shaped potential.

Figure 1 displays the surface potentials for Ne, Ar, Kr and Xe on copper used in the molecular dynamics simulations. The well depths for Ar, Kr and Xe are of the same order as the binding energies found by Engel and Gomer (1969) for these gases on a Tungsten surface (≈ 0.1 eV) and are in approximately the same ratio. The potentials have the same universal shape as that proposed by Vidali (1983).

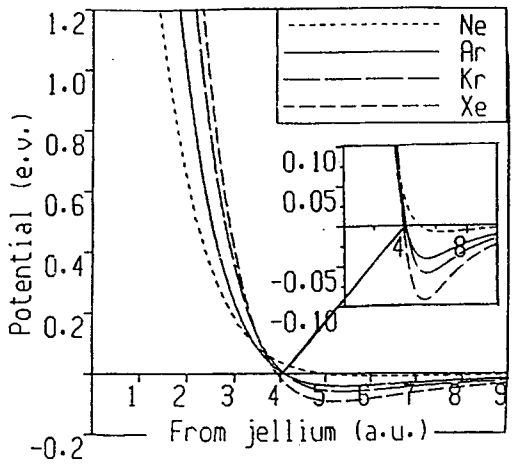

Figure 1. The potentials for a Ne, Ar, Kr and Xe atoms on a copper surface as used in the molecular dynamics simulations.

4. Wavefunction calculations

4.1. Puska–Nieminen method

For bubbles with radii less than about 12 Å it is possible to use the method of Puska and Nieminen (1983). This method divides the bubble and a volume of crystal (we have actually used jellium) around the bubble into a linear mesh, the potential and electron density at each point then being found by the superposition of free atom densities and potentials. So for regions in the bubble which are in the image potential region of the metal the potential is given by

$$V(\boldsymbol{r}) = \sum_i V_{\mathrm{at}}^i(|\boldsymbol{r} - \boldsymbol{R}_i|) + \sum_i V_{\mathrm{pol}}(|\boldsymbol{r} - \boldsymbol{R}_i|) + V_i(\boldsymbol{r}) \tag{9}$$

where V_{at} is the electrostatic potential of the atom found from Hartree–Fock tables (Fischer 1972), V_i is the image potential of the metal (see equation (30)) and V_{pol} is the potential due to the polarization of the gas atoms given by Schrader (1979) to be

$$V_{\mathrm{pol}}(r) = \begin{cases} -\beta/r^4 & \text{if } r \geq r_0 \\ -\beta/r_0^4 & \text{if } r < r_0. \end{cases}$$

Schrader's values for β and r_0 for each gas are given in table 2.

For all other regions within or near the host, the potential is given in the approximation of an effective potential (see equation (28))

The three-dimensional Schrödinger equation is then differenced and solved numerically using a Gauss–Seidel over-relaxation technique.

This method was applied only for the high density limit of each gas in order to check that any deviations of the positron away from a perfect surface state predicted by the pseudopotential calculation would also present in the more lengthy Puska–Nieminen calculation. It was assumed that the gas atoms were arranged in a FCC structure (this being the best representation of the average distribution of atoms in the void

at these high densities found by the molecular dynamics simulations) and the gas atoms nearest the jellium where placed at a distance from the jellium corresponding to the first peak of the molecular dynamics simulation found for that density by a combination of adjusting the cavity size and plucking away atoms from the crystal closer to the jellium than this distance.

4.2. Pseudopotential method

We will only briefly outline the pseudopotential method here; more detailed accounts of the method and its variations are given by Mijnarends (1983) and Stott and Kubica (1975).

The Schrödinger equation is split into two parts by defining the real wavefunction to be the product of a slowly varying envelope or 'pseudo-wavefunction' Ψ_p and a short range wavefunction $\Upsilon(r)$ which may be chosen to be the solution of the Schrödinger equation in a single Wigner–Seitz sphere around a given type of atom.

Υ and Ψ_p satisfy the equations

$$-\nabla^2\Upsilon(r) + V_{WS}(r)\Upsilon(r) = E_{WS}\Upsilon(r) \tag{10}$$

$$-\nabla^2\Psi_p(r) + V_p(r)\Psi_p(r) = E\Psi_p(r) \tag{11}$$

where $V_{WS}(r)$ is a Wigner–Seitz potential. The equations are related via V_p, which is termed the effective or pseudopotential.

$$V_p(r) = \begin{cases} E_{WS} - 2(\mathrm{d}\log_e \Upsilon(r)/\mathrm{d}r)\nabla & \text{if } r < r_{WS} \\ V(r) & \text{if } r \geq r_{WS}. \end{cases} \tag{12}$$

The effect of the log term on the pseudo-wavefunction is small, particularly in the noble gases where both Υ is flat over the majority of the Wigner–Seitz cell (see subsection 5.2) and Ψ_p varies slowly. We will therefore neglect it as is the normal practice in surface and void calculations (see for example Nieminen and Manninen 1979) for a review of pseudopotential methods used in this type of problem and the validity of dropping the log term). We therefore do not solve for $\Psi_p(r)$ cell by cell, but in the approximation of spherical symmetry in a potential which must go to $-\phi_+$ (ϕ_+ being the positron workfunction) in both the host metal and the trapped gas. We do this by rescaling the ordinary potentials associated with the surface, the correlation, image and electrostatic potentials, so that they approach the desired limits for the bulk metal and bulk gas. Rescaling in this fashion for pure surface states was first done by Brown *et al* (1987).

In spherical symmetry equation (11) may be rewritten as

$$-\frac{\mathrm{d}^2U(r)}{\mathrm{d}r^2} + V_p(r)U(r) + \frac{l(l+1)}{r}U(r) = EU(r) \tag{13}$$

where the positron was as usual taken to be in an s state and $U(r)$ and $\Psi_p(r)$ are related by

$$U(r) = (4\pi)^{1/2}\Psi_p(r)r \tag{14}$$

4.3. The Wigner–Seitz method

The Wigner–Seitz method involves solving numerically the spherical Schrödinger equation

$$-\frac{d^2\Xi(r)}{dr^2}+V(r)\Xi(r)+\frac{l(l+1)}{r}\Xi(r)=E\Xi(r)\,. \tag{15}$$

The positron is assumed to be in an s state and Υ must be normalized to 1 in a sphere having the volume occupied by a single atom of the assumed FCC crystalline gas so

$$\Xi(r)=(4\pi)^{1/2}\Upsilon_n(r)r\,. \tag{16}$$

The radius of the Wigner–Seitz sphere is therefore given by

$$r_{WS}=\left(\frac{3}{4\pi\rho_{gas}}\right)^{1/3} \tag{17}$$

where ρ_{gas} is the number of gas atoms per unit volume (in atomic units). The equation being solved subject to the boundary condition

$$d\Upsilon(r_{WS})/dr_{WS}=0\,. \tag{18}$$

A potential

$$V(r)=V_e(r)+V_{pol}(r)+\sum_i V_{pol}(|\boldsymbol{r}-\boldsymbol{R}_i|) \tag{19}$$

is employed where $V_e(r)$ is the electrostatic potential

$$V_e(r)=\frac{2Z}{r}-\int_{r<r_{WS}}\frac{2\rho_-(\boldsymbol{r}')}{|\boldsymbol{r}'-\boldsymbol{r}|}\,d\boldsymbol{r}'-\frac{2}{r_{WS}}\int_{r'>r_{WS}}\rho_-(\boldsymbol{r}')\,d\boldsymbol{r}' \tag{20}$$

where the last term is a small correction term which assumes that the number of electrons outside of the Wigner–Seitz sphere radius (being equal to the number of electrons gained from neighboring atoms) are concentrated at the sphere radius. The third term in equation (19) assumes that the correlation potential due to the atoms around the Wigner–Seitz sphere may be well represented by

$$\sum_i V_{pol}(|\boldsymbol{r}-\boldsymbol{R}_i|)\approx-\frac{\beta N}{2Rr}\int_{R_n-r}^{R_n+r}\frac{ds}{s^3}-\frac{2\beta\pi\rho_{gas}}{r}\int_{R_n}^{\infty}\int_{R-r}^{R+r}\frac{R\,ds\,dR}{s^3} \tag{21}$$

where R is the radius of an elementary shell from the centre of the sphere, s is the distance from the point r to an annulus on the shell, N the co-ordination number and R_n the distance to the N nearest neighbours. The expression reduces after a little manipulation to

$$\sum_i V_{pol}(|\boldsymbol{r}-\boldsymbol{R}_i|)\approx-\frac{N\beta}{(R_n^2-r^2)^2}+4\pi\rho_{gas}\beta\left[\frac{R_n}{2(r^2-R_n^2)}+\frac{1}{4r}\log_e\left(\frac{R_n-r}{R_n+r}\right)\right]. \tag{22}$$

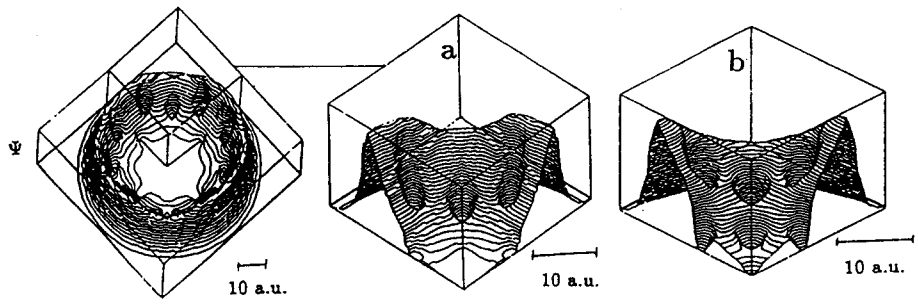

Figure 2. Positron wavefunction as calculated using the Puska–Nieminen method in jellium in a bubble of Xenon at a density of (*a*) 2×10^{-3} atoms au^{-3} and (*b*) 3.0×10^{-3} atoms au^{-3} showing the gradual deviation of the positron from a perfect surface state due to the polarization potential of the xenon.

4.4. Normalization

The function $\Upsilon_n(r)$ (the Wigner–Seitz wavefunction normalized to one in the Wigner–Seitz cell) must be renormalized such that the value of $\Upsilon_{rn}(r_{WS})$ is the same for both the host and the contained gas which ensures that $d(\Upsilon_{rn}(r_{WS})\Psi_p(r_{WS}))/dr$ is a smooth and continuous function at all points (Stott and Kubica 1975). We are free to chose $\Upsilon_{rn}(r_{WS})$ to be what we wish and have chosen it to be equal to 1 as this means that for regions where $\Upsilon_{rn}(r) = 1$ (at the surface of the metal for example), $\Psi_p(r) = \Psi(r)$, which is convenient for evaluating annihilation rates with the free electrons of the metal.

The entire wavefunction must then be normalized. To a first approximation we may assume that $\Upsilon_{rn}(r) = 1$ at all points, and as such the normalization constant will simply be the integral of the pseudo-density. An improvement on this approximation is to assume that $\Psi_p(r)$ varies slowly and smoothly over the regions where $\Upsilon_{rn}(r) < 1$ such that it may be considered to have either a constant, or good average value (see figure 2). The normalization constant will then be given by

$$N \approx \int_0^\infty |U(r)|^2 \, dr - \sum_i^{\text{Atom}} \sum_j^{\text{Cells}} |\Psi_p(r_j)|^2 \left(\frac{4\pi r_{WS_i}^3}{3} - \int_{\text{cell}} |\Upsilon_{rn}(r_i)|^2 \, dr \right) \tag{23}$$

where $\Upsilon_{rn}(r)$ is the renormalized Wigner–Seitz wavefunction and the summations are over the i types of atom and j cells of each type of atom. The value of $\Upsilon_n(r_{WS})$ in He as a function of gas density is given by Dunn *et al* (1990a) as

$$\Upsilon_n(r_{WS}) = \sqrt{1/(\rho_{gas}^{-1} - \eta)}\,. \tag{24}$$

This relationship turns out to also be the case in the other noble gases (see section 4) and values for η in each gas are given in table 2. Equation (23) may then be simplified if it is noted that

$$\int_{\text{cell}} |\Upsilon_{rn}(r)|^2 \, dr = \frac{1}{|\Upsilon_n(r_{WS})|^2} \tag{25}$$

where $\Upsilon_n(r_{WS})$ is the value of the Wigner–Seitz wavefunction normalized to 1 in the cell at the sphere radius. Making use of equations (24) and (25) we may rewrite (23)

in the approximation of a continuously varying density as

$$N \approx \int_0^\infty |U(r)|^2 \, \mathrm{d}r - \sum_i^{\text{Atom}} \int_0^\infty |U(r)|^2 \eta \rho_i(r) \, \mathrm{d}r \,. \tag{26}$$

η may be interpreted as a 'missing volume', the sum of all the $|\Psi_p|^2\eta$ may therefore be seen as the amount that must be taken off the integral of the pseudo-density to obtain the integral of the real positron density, figure 3 should make this clear.

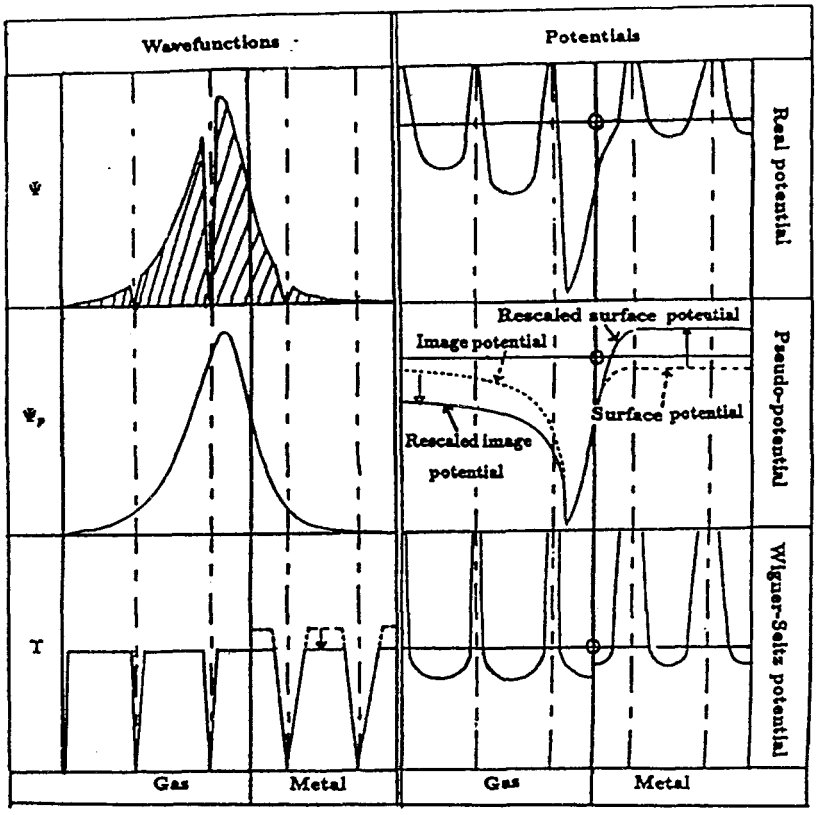

Figure 3. Schematic illustration of the potentials and wavefunctions used in the pseudopotential method. The real wavefunction (top) is the product of the renormalized Wigner–Seitz wavefunctions (bottom) with the pseudo-wavefunction (middle). The Wigner–Seitz wavefunctions may be thought of as flat with a 'missing volume', η, around the nucleus. The metal and gas Wigner–Seitz wavefunctions must be matched (illustrated by the arrow in the metal Wigner–Seitz wavefunction) so that the real function is a smooth and continuous function.

4.5. The potential

The effective potential V_p may be split into two parts, the potential of the host metal, and the image potential of the host along with the potential of the gas in the bubble. Each part of the potential must be formed so that it approaches in the jellium the

positron energy in the host, and in the bubble, the positron's average energy in the gas at a given density.

The dipole (electrostatic) potential and correlation potential are well approximated by

$$V_d(z) = \left[\frac{3\pi^2 n_0}{(\exp(zF/\lambda_F)+1)}\right]^{2/3} - [0.5 + \exp(-0.9r_s)] \tag{27}$$

where the first term is the electrostatic potential in the Thomas–Fermi approximation using the Lang-Kohn electron densities of equation (3), and the second term is a parametrization of the correlation energy of Bhattacharyya and Singwi (1982). This potential will have the correct 'form' but will not have the correct limit in the metal. However by altering the scale of the potential (rescaling) we may arrange for the correct limit to be achieved, figure 3 illustrates this, showing the dipole potential and rescaled dipole potential. Following Brown *et al* (1987) we have rescaled V_d so that the new scale goes from the limit of the correlation energy (−0.5 Ryd) outside the jellium and to the positron energy in the jellium ($-\phi_+$), the rescaled potential is therefore

$$V_{p-h}(z) = A(V_d(z) + 0.5) - 0.5 \tag{28}$$

where A is the rescaling factor

$$A = \frac{(0.5 - \phi_+)}{(0.5 + V_d(-\infty))}. \tag{29}$$

The work function of Cu is ≈ -0.95 eV (Hodges and Stott 1973).

The image potential is of course given by

$$V_i(z) = -[2(z - z_m)]^{-1} \tag{30}$$

where z_m is the shift of the mirror plane caused by the positron given by Lang and Norskov (1983). In the same way as was done for the host we must now rescale the image potential to go to the limit of the positron energy in the gas of the density being considered.

The image potential may now be rescaled so that the effective potential will be given by

$$V_{p-i}(z) = \frac{(0.5 - \phi_{gas})}{0.5}(0.5 + V_i(z)) - 0.5. \tag{31}$$

The crossover point z_0 where V_{p-h} turns into V_{p-i} is decided by the condition

$$V_{p-h}(z_0) = V_{p-i}(z_0). \tag{32}$$

4.6. Calculation of lifetimes

4.6.1. Annihilation in the noble gas Wigner–Seitz cell. If the average momentum of a positron with respect to the gas atom is known, a constant average enhancement factor for the atom may be used to obtain the annihilation rate so that the annihilation rate can be expressed in the form

$$\lambda(r) = \pi r_0 c^2 \overline{\gamma} |\Upsilon(r)|^2 n(r) \tag{33}$$

where $\overline{\gamma}$ is the average enhancement factor at the mean positron momentum. Alternatively, we may write

$$\lambda = \pi r_c^2 c Z_{\text{eff}} \rho_{\text{gas}} \tag{34}$$

where Z_{eff} is the effective number of electrons per atom. Values for Z_{eff} have been calculated for Ne, Ar, Kr and Xe by McEachran *et al* (1978, 1979, 1980). All such values are found to be relatively constant for values of wavenumber $K > 0.02$ au^{-1} and so provided that we are confident that our positron has a mean wavenumber well above this value we may with very little loss of accuracy use the same constant enhancement factor for all our calculations. This is indeed the case for positrons in bubbles where the positron is trapped in a surface potential well and has a wavenumber greater than 0.02 au^{-1} with respect to the gas atom.

The total annihilation rate in the Wigner–Seitz sphere will therefore be given by

$$\lambda = \pi r_0^2 c \overline{\gamma} \left(\int_0^{r_{\text{WS}}} |\Upsilon_n(r)|^2 n(r) 4\pi r^2 \, \mathrm{d}r + |\Upsilon_n(r_{\text{WS}})|^2 \int_{r_{\text{WS}}}^{\infty} n(r) 4\pi r^2 \, \mathrm{d}r \right). \tag{35}$$

(The correction term in equation (35) amounts to between 0 and 4% of the total annihilation rate). For the purposes of these calculations $\overline{\gamma}$ was found by equating the annihilation rate calculated at the solid uncompressed density of the gas with one found by experiment. For this we have used the values given by Haberl and Douglas (1979) for Ne and Ar and the values given by Liu and Roberts (1963) for Xe. There is as yet no experimental value for krypton and so we have used the estimate of Hansen, Nieminen and Puska (1983). The values of the average enhancement factors used are given in table 2.

4.6.2. Annihilation from the surface. For the purposes of these calculations we have assumed the positron to be in a simple, perfect surface state, the positron being extended over the entire surface. The annihilation rate with the surface free electrons is determined in the Brandt–Reinheimer (1977) approximation with a cut-off in the evaluation for $z > z_0$ (Nieminen *et al* 1984), z being the distance from the jellium edge and where z_0 is given in equation (32). (Recently, several more complex models have been proposed in order to explain the unobserved anisotropy which is expected in angular correlation curves due to the positrons anisotropy in momentum parallel and perpendicular to the surface. See for example Brown *et al* (1988) in which the possibility of positrons being trapped at surface defects is investigated, and Jensen and Walker (1988) in which there is a thorough treatment of correlation effects in strongly inhomogeneous environments.)

$$\lambda_{n\_}(z) = \begin{cases} (2 + 134 n\_(z)) \times 10^9 & \text{if } z \le z_0 \\ 0 & \text{if } z > z_0. \end{cases} \tag{36}$$

4.6.3. Total annihilation rate. The core annihilation rate off a single atom in the local approximation is the integral of the product of the positron density and the electron density. As the positron wavefunction is the product of the pseudo-wavefunction and the renormalized Wigner–Seitz wavefunction, the core annihilation rate will be given by

$$\lambda_{\text{atom}} = \frac{\pi r_c^2 c\overline{\gamma}}{N|\Upsilon_n(r_{\text{WS}})|^2} \int |\Psi_p(\boldsymbol{r})\Upsilon_n(\boldsymbol{r})|^2 n(\boldsymbol{r})\,\mathrm{d}\boldsymbol{r} \tag{37}$$

where r is the distance from the atom nucleus and $n(r)$ is the core electron density and $\overline{\gamma}$ is the average enhancement factor. When Ψ_p may be considered to be flat, or to have a good average value across the cell we may assume that the annihilation rate from a single atom will be given by

$$\lambda_{\text{atom}} = |\Psi_p|^2 \lambda_{\text{WS}}/N|\Upsilon_n(r_{\text{WS}})|^2 . \tag{38}$$

The total annihilation rate will be the sum of the contributions from the j cells of each atom type i and the annihilation rate off the free electrons where the free electron density is given by the parametrized Lang-Kohn surface electron densities.

$$\lambda_{\text{total}} = \sum_i^{\text{atom}} \sum_j^{\text{cell}} \frac{|\Psi_p(\boldsymbol{r}_j)|^2)\lambda_i}{N\Upsilon_i(r_{\text{WS}})|^2} + \frac{1}{N} \int |\Psi_p(\boldsymbol{r})|^2 \lambda_{n\_}(\boldsymbol{r})\,\mathrm{d}\boldsymbol{r} . \tag{39}$$

As we are dealing with continuous densities and do not have knowledge of the exact cell positions, we convert the discrete summation into a continuous one so that total annihilation rate will be

$$\lambda_{\text{total}} = \sum_i^{\text{atom}} \int_0^\infty \frac{|U(r)|^2 \rho_i(r)\lambda_i}{N|\Upsilon_i(r_{\text{WS}})|^2}\,\mathrm{d}r + \frac{1}{N}\int_0^\infty |U(r)|^2 \lambda_{n\_}(r)\,\mathrm{d}r . \tag{40}$$

In copper the total bulk rate is $\lambda \approx 8.2\ \text{ns}^{-1}$ (Mackenzie (1983); taking the free electron rate ($\approx 3.8\ \text{ns}^{-1}$) away from this we estimate the bulk core rate to be $\lambda_{\text{core}} = 4.4\ \text{ns}^{-1}$ and the annihilation rate λ_{gas} with the noble gas core electrons will be given in equation (42) as a function of gas density (for which we use the average gas density in the void).

5. Results

5.1. Results from molecular dynamics simulations

The molecular dynamics simulations were performed on gases up to a density equivalent to a pressure of the order 0.5×10^9 Pa at 300 K (Ronchi 1981). This is equivalent to bubbles of radius of about 10 Å (assuming thermal equilibrium such that the relationship $P = 2\gamma/r$ holds).

The profiles away from the jellium exhibited a high degree of ordering above the gas's solid uncompressed density but below this density they became more fluid with a noticeable peak above the surface potential well, the second and third peaks falling off in size exponentially. An increase of pressure caused the first peak to be pushed in towards the jellium. The total movement of the position of the first peak from the lowest to the highest pressure was about 1.5 au for each gas.

Figure 4 shows typical density profiles for each gas at four different densities.

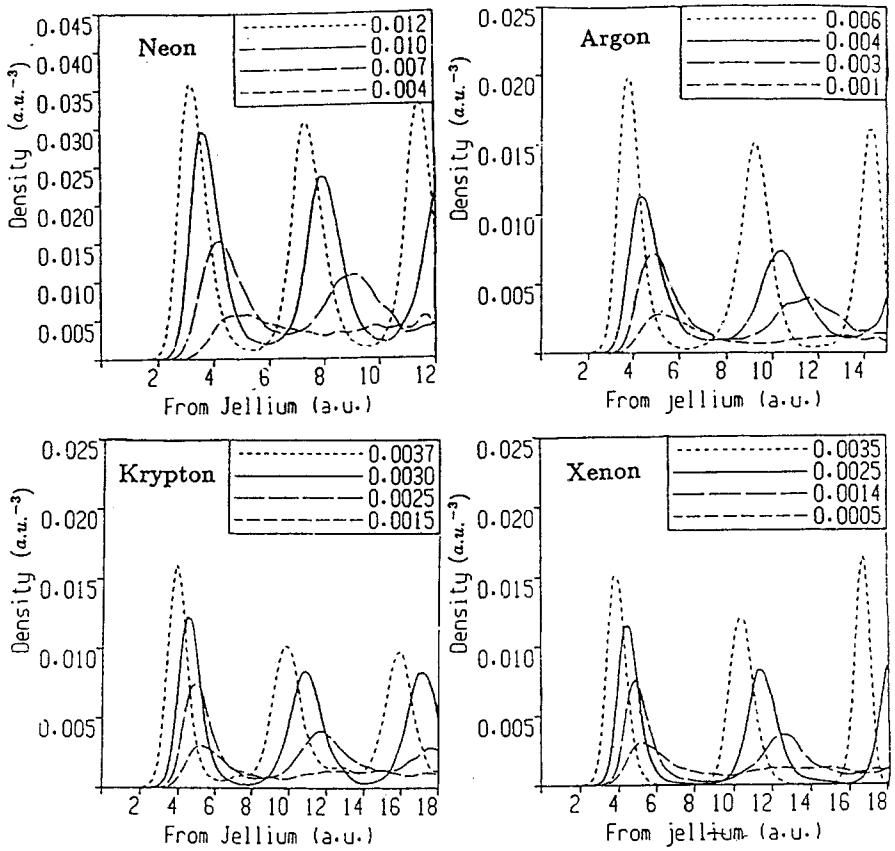

Figure 4. Typical output from molecular dynamics simulations at four different densities for each gas at 300 K.

5.2. Results of Wigner–Seitz calculations and comparison with experiment

The wavefunctions for all the gases were found to be predominantly flat, being depleted locally around the nucleus of the atom. The wavefunction at the Wigner–Seitz sphere radius as a function of density was found to be well represented by the relationship

$$\Upsilon(r_{\mathrm{WS}}) = \sqrt{1/(\rho_{\mathrm{gas}}^{-1} - \eta)} \tag{41}$$

where values for η are given in table 2. Using the constant average enhancement factors given in table 2, the annihilation rate was in each case a linear function of the gas density given by

$$\lambda = A\rho_{\mathrm{gas}} \times 10^9 \quad \mathrm{s}^{-1} \tag{42}$$

where the density is in atomic units, or

$$\lambda = \pi r_{\mathrm{c}}^2 c Z_{\mathrm{eff}} \rho_{\mathrm{gas}} \quad \mathrm{s}^{-1} \tag{43}$$

in SI units. Values for Z_{eff} are given in table 2. The positron work function ϕ_+, was also found to be a linear function of the gas density. The work function is given in units of eV by

$$\phi_+ = B\rho_{\text{gas}} \tag{44}$$

Values for B are also in table 2. The linearity of the work function for argon is not as good as the other gases and is better described below 0.002 atoms au^{-3} by the binding energy as given by the optical potential in the low density limit (Hansen *et al* 1984)

$$E \approx 4\pi\rho_{\text{gas}}d \tag{45}$$

where d is the scattering length and energy is in units of Ryd.

5.3. Comparison with experiment

Gullikson and Mills Jr (1988) have reported experimental values of binding energies of 1.55, 2.0 and 2.3 eV for solid uncompressed Ar, Kr and Xe respectively. These values are somewhat smaller than the values of 2.0, 2.4 and 3.1 eV found using the Puska–Nieminen method (Hansen *et al* 1983) and 2.2, 2.5 and 3.4 eV found by us using the Wigner–Seitz method.

The discrepancy between experimental and theoretical values is not unusually large for positron work functions. The consistently lower experimental values do however, lead us to suspect that the practice of using 'free atom' polarization potentials in the solution of this type of problem may be a possible source of error and so should be reconsidered.

5.4. Results for positron wavefunction and surface annihilation

The positron wavefunctions and the resulting annihilation rates in empty voids were found to be independent of the void size above a radius of 20 au and the calculations of the positron wavefunctions were always carried out in bubbles above this size (usually about 30 to 40 au).

The surface annihilation rates were, as a result of the change in the wavefunction caused by the presence of the gas, a function of the gas density (and hence of the gas's work function), they are well parametrized by the Fermi–Dirac-type relationship

$$\lambda_{\text{surf}} = \lambda_{\max}[\exp(-3.5 + \phi_+) + 1]\,. \tag{46}$$

The deviation of this rate from a perfect surface state rate is small in neon (about 10%) at the highest densities. In argon and krypton the reduction is greater at high densities (about 25%). In the case of xenon the reduction is very marked, being about 60% at a density of 3×10^{-3} atoms au^{-3} equivalent to a pressure of 2.8×10^9 Pa and bubble radius of 22 au (Ronchi 1981). This deviation of the positron wavefunction in xenon is displayed in figure 2 where the calculation has been performed by the Puska–Nieminen method lending weight to the results of the pseudopotential calculations.

The experimental annihilation rate for copper is $\lambda = 2 \pm 0.13$ ns^{-1} (Kögel *et al* 1979) for voids (we are unaware of an experimental external surface rate) as compared with our value of $\lambda = 1.66$ ns^{-1}. We have no reason to offer for this discrepancy, though it does appear to be the case that external surface annihilation rates are about 15% less than internal surface (void) rates (Jensen and Nieminen 1987).

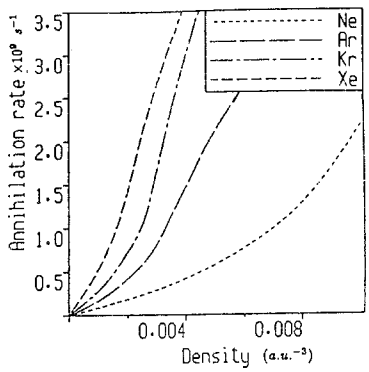

Figure 5. Annihilation rates off the core electrons of the Noble gases in bubbles of Ne, Ar, Kr and Xe.

Table 3. The constants C and D in equations (47) and (48) and the range of binding energies, BE, of the positron over the range of densities considered.

Gas	C	D	BE (eV)
Ne	33000	24000	2.9–3.47
Ar	58000	40000	2.9–3.8
Kr	85000	55000	2.9–3.9
Xe	118000	70000	2.9–4.0

5.5. Annihilation with the gas

The annihilation rate as a function of gas density increased more than linearly with gas density, this being caused primarily by the decrease in distance of the first peak of the gas density profile from the jellium with increase of pressure. In the case of the heavier gases which had large correlation potentials, there was an additional increase due to the deviation of the positron wavefunction into the gas away from the perfect surface state.

Figure 5 displays the annihilation rates of each gas as a function of density.

5.6. Total lifetime

Adding together the surface and gas contributions to the bubble annihilation rate produces an almost linear dependency of lifetime on density. To a reasonable approximation the lifetimes of the bubble state are given by

$$\tau = 600 - C\rho_{\text{gas}} \quad \text{ps} \tag{47}$$

where values for C are given in table 3. We note at this point, in view of the concern we expressed in subsection 5.3 over the use of Schrader's free atom polarization potentials in the evaluation of the binding energies of the gases, that calculations with the gas pseudopotential switched off yield results very little different to the results with the potential on. This is because any loss in the surface annihilation rate caused by extension of the positron into the gas is almost exactly compensated for by the increase of annihilation with the gas. As such, the accuracy of the evaluation is fortunately not sensitive to minor inaccuracies in the gas pseudopotential.

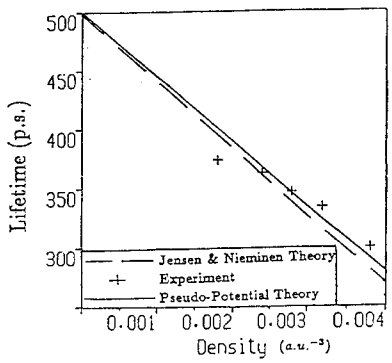

Figure 6. Theoretical and experimental annihilation rates of a positron in a bubble of Krypton as a function of density compared with the results of Jensen and Nieminen.

5.7. Comparison with experiment

Experimental positron annihilation investigations of noble gas bubbles in metals seem to have been thus far confined to helium and krypton. In the case of krypton, Jensen *et al* (1988) determined positron annihilation rates as a function of gas density using densities found by transmission electron microscopy. Our theoretical results yield slightly longer lifetimes, but this discrepancy is due entirely to the use of theoretical rather than experimental surface annihilation rates which as mentioned previously are known to be smaller. Use of an experimental surface annihilation rate of 2 ns^{-1} along with the relationship in equation (46) yields

$$\tau = 500 - D\rho_{\text{gas}} \quad \text{ps} \tag{48}$$

where the values for D are given in table 3. This brings the pseudopotential method into excellent agreement with the Jensen–Nieminen method whose value for D for krypton is 62 704 as compared with our value of 55 000. Our theoretical lifetime-density relationship for krypton is compared with the experimental results of Jensen *et al* (1988) in figure 6.

6. Conclusions

We have calculated the binding energies, positron wavefunctions and annihilation rates in the noble gases Ne, Ar, Kr and Xe as a function of density. The values of the positron work function found in this way and using the Puska–Nieminen method were generally larger than those found by Gullikson and Mills Jr. experimentally using LEPD. This has lead us to believe that the use of free atom polarization potentials for this type of calculation may have to be reconsidered.

The use of pseudopotentials in the calculation of annihilation rates in bubbles has produced results in substantial agreement with experiment and with the more lengthy Jensen-Nieminen method in the case of krypton. The results of such calculations were found to be relatively insensitive to the effective potential used for the contained gas and so the total annihilation rate for a bubble containing gas at a given pressure should be accurate despite our concern over the use off free atom polarization potentials.

For all gases at intermediate pressures the positron was found to be in a stable surface state. In the cases of Ne, Ar and Kr at high pressures, the wavefunction was

found to be attracted slightly into the bubble reducing the surface annihilation rate, but increasing the gas annihilation rate by almost the same amount. In the case of xenon, the wavefunction was found to deviate substantially away from the pure surface state at high pressure but the wavefunction was still greatest over the surface potential.

In summary, we have shown that pseudopotential calculations for positron annihilation in this type of defect, provide a fast, efficient and accurate alternative to the Jensen-Nieminen method of calculation. Our calculations for the previously unanalysed gases Ne, Ar and Xe, show that positron annihilation techniques will provide an invaluable tool in the analysis of metals defected with bubbles of any noble gas.

References

Bhattacharyya P and Singwi K S 1972 *Phys. Lett.* **41A** 457

Bernardes N 1958 *Phys. Rev.* **112** 1534

Brandt W and Reinheimer J 1971 *Phys. Lett.* **35A** 109

Brown A P, Walker A B and West R N 1987 *J. Phys. F: Met. Phys.* **17** 2491

Dunn G M, Rice-Evans P and Evans J H 1990 *Radiat. Eff. Def. Solids* at press

—— 1990 *Phil. Mag.* at press

Engel T and Gomer R 1969 *J. Phys. Chem.* **52** 5572

Evans J H 1985 *Phys. Bull.* **36** 58

—— 1986 *Nucl. Instrum. Methods* B **18** 16

Fischer C F 1972 *At. Data Nucl. Data Tables* **4** 301–99

Gullikson E M and Mills Jr A P 1988 *Phys. Rev.* B **37** 588

Hansen H E, Nieminen R M and Puska M J 1984 *J. Phys. F: Met. Phys.* **14** 1299

Hautojärvi P, Rytsölä K, Tuovinen P, Vehanen A and Jauho P 1977 *Phys. Rev. Lett.* **38** 842

Hockney R W and Eastwood J W 1983 *Computer Simulations Using Particles* (New York: McGraw-Hill)

Hodges C H and Stott M J 1973 *Phys. Rev.* B **7** 73

Jensen K O 1988 *Def. Diffus. Forum* **57–58** 207

Jensen K O and Nieminen 1987 *Phys. Rev.* B **36** 8219

Jensen K O, Eldrup M, Pedersen N J and Evans J H 1988 *J. Phys. F: Met. Phys.* **18** 1703

Jensen K O and Walker A B 1988 *J. Phys. F: Met. Phys.* **18** L277

Kögel, G Winter J and Triftshäuser W 1979 *Positron Annihilation, ICPA5* (Japan Institute of Metals) p 707

Lang N D and Kohn W 1973 *Phys. Rev.* B **7** 3541

Lang N D and Norskov J K 1983 *Phys. Rev.* B **27** 4612

Mannienen M, Norskov J K, Puska M J and Umrigar C 1984 *Phys. Rev.* B **29** 2314

Mackenzie I K 1983 *Positron Solid State Physics (Proc. Int. School of Physics)* (Amsterdam: North-Holland) p 204

March N H 1957 *Adv. Phys.* **61** 1

Mijnarends P E 1983 *Positron Solid State Physics (Proc. Int. School of Physics)* (Amsterdam: North-Holland) p 161

Mills Jr A P 1979 *Solid State Commun.* **31** 623

Nieminen R M 1989 *Proc. 8th Int. Conf. on Positron Annihilation, Gent 1988* (Singapore: World Scientific) p 60

Nieminen R and Manninen MJ 1979 *Positrons in Solids (Springer Topics in Current Physics)* ed P Hautojärvi (Berlin: Springer) p 145

Nieminen R, Puska M J and Manninen M 1984 *Phys. Rev. Lett.* **53** 1298

Norlander P and Harris J 1984 *J. Phys. C: Solid State Phys.* **17** 1141

Plumer M L and Stott M J 1985 *JPC* **18** 4143

Puska M J and Nieminen R M 1983 *J. Phys. F: Met. Phys.* **13** 333

Ronchi C 1981 *J. Nucl. Mater.* **96** 314

Schrader D M 1979 *Phys. Rev.* A **20** 918

Stott M J and Kubica P 1975 *Phys. Rev.* B **11** 1

Stott M J and Zaremba E 1979 *Solid State Commun.* **32** 1297
Ullmaier H 1983 *Proc. Int. Symp. on Helium in Metals, Julich 1982 (Radiat. Eff. Def. Solids)* **78**
Vidali G, Cole M W and Klein J R 1983 *Phys. Rev.* B **28** 3064
Zaremba E and Kohn W 1975 *Phys. Rev.* B **13** 2270